Three Dimensional Modeling

Modeling three dimensional tissue scaffold using functional representation

S.Lakshmi Piriya,
Department of Computer Science,
Research Scholar (Bharathiar University),
Assistant Professor, Mohamed Sathak College of Arts and Science, Chennai, India.
lakshmi.piriya.s@gmail.com
Mobile: 9789972221

Dr.S.K.Mahendran,
Director, SVS Institute of Computer Applications,
Anna University,
Coimbatore, India.
sk.mahendran@yahoo.co.in

***Abstract*— Most of the objects in modern computer graphics are mostly represented by boundary representation models like polygonal meshes. Such models only store information about an object's boundary and are relatively easy to render and often highly scalable. While this is sufficient for a variety of applications like many types of computer animation and games, other uses require information about volume rather than just surface. Functional representation allows defining objects as a set of geometric primitives with certain operations and relations. Function based modeling of lattice scaffold is discussed using the microstructure data obtained with magnetic resonance imaging (MRI).**

Keywords: microstructure, lattice, tissue engineering, scaffold, functional representation, digital fabrication.

I. INTRODUCTION

In the visual effects and games industry, the predominant modeling techniques are using polygonal meshes. While these offer various benefits and are well integrated into current pipelines, they only represent surfaces and have a given amount of detail. As a consequence, information about an object's internal structure cannot be stored and modeling of heterogeneous real-world objects is difficult. In other fields like Computer Aided Design and Three Dimensional printing, the tradeoffs cannot be circumvented without effort and alternative representations are needed [R.1]. One alternative is to use "Functional Representation (FRep) in geometric modeling" as suggested by Pasko et al. (1995) [R.2]. The so-called FRep allows the definition of objects, operations and relations as a mathematical function as opposed to point data and meshes. In this work, we concentrate on modeling regular microstructure known as lattice. By "lattice" we mean a periodic spatial structure consisting of crossing rods, laths or other thin strips of material [R.2].

II. PRIOR WORK

A. Overview of Representations

The most dominant way of representing objects in modern computer graphics are boundary representation models, also known as BRep [R2]. Such models do not store any information about object's inner properties. Figure I shows a triangle mesh, a popular type of a boundary representation model. In film and games, most efforts are spent on creating visually pleasing results rather than accurate models of reality. Therefore, boundary representation are often sufficient and even preferred because they offer a rich set of operations and are comparatively easy to render [R.4]. For other purposes, volumetric representations as in Figure 2 allow us to store the object's internal structure rather than only limited surface information. This is especially important when modeling real-life heterogeneous objects. There are a number of volumetric representations including voxel representation, implicit surfaces and FReps.

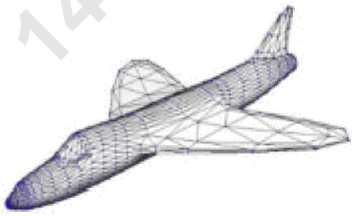

Figure 1: Example of a boundary representation: triangle mesh model [R.3].

Figure 2: Example of a boundary representation: triangle mesh model [R.3].

B. The Functional Representation(FRep)

The Functional Representation (FRep) combines different models such as algebraic surfaces; skeleton based "implicit" surfaces, CSG (Constructive Solid Geometry), sweeps, volumetric objects, parametric models and procedural models. The representation defines a geometric object by a single real continuous function of point coordinates as $F(X) \geq 0$ (Pasko 2011) [R.2]. This also lets us represent models independent

from resolution. A constructive tree defines functions and provides a visual overview of operations and parameters. Leaf nodes are primitives like a box, sphere, torus, etc. Non-leaf nodes contain operations and relations. This functionality was implemented and made accessible via a FRep API.

One particular class of the FRep operations is set-theoretic ones defined by Real functions [R.2]. An object resulting from the set-theoretic operations has the defining function expressed as follows:

$f3 = f_1 \vee f_2$ for the union

$f3 = f_1 \wedge f_2$ for the intersection

$f3 = f_1 \setminus f_2$ for the subtraction

Where f_1 and f_2 are defining functions of initial objects, f3 is the final object obtained and the symbols ∧,∨, / are signs of Real functions. Figure 3 shows sample models and related graphs obtained by using the above set-theoretic operations.

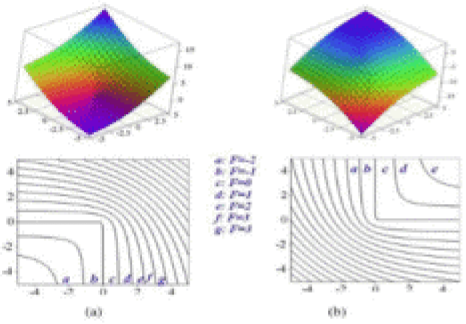

Figure 3: Set-theoretic operations based on Real functions: (a) Union and (b) Intersection (Kravtsov 2011) [R.2]

III. MODELING OF LATTICE MICROSTRUCTURE

We propose the following approach to model infinite regular 3D lattices:

Step 1: A set of infinite parallel slabs orthogonal to each coordinate axis can be defined by a corresponding periodic function; to define the infinite slabs, the following functions can be applied:

$$s_x(x, y, z) = \sin(q_x x + p_x) - l_x \quad (1)$$

$$s_y(x, y, z) = \sin(q_y y + p_y) - l_y \quad (2)$$

$$s_z(x, y, z) = \sin(q_z z + p_z) - l_z \quad (3)$$

where the inequality $s_x \geq 0$ describes a set of slabs orthogonal to x-axis and parallel to each other, the frequency q_x defines the distance between parallel slabs along x-axis, the phase p_x defines the position of slabs on the x-axis relative to the origin, and the threshold $-1 < l_x < 1$ together with the frequency defines the thickness of each slab. The slabs orthogonal to y and z axes are symmetrically defined by the functions s_y and s_z.

Step 2: The intersection of two of these sets results in the infinite rods parallel to one of the axes;

$$r_x(x, y, z) = s_y \wedge_\alpha s_z \quad (4)$$

$$r_y(x, y, z) = s_x \wedge_\alpha s_z \quad (5)$$

$$r_z(x, y, z) = s_x \wedge_\alpha s_y \quad (6)$$

Here the inequality $r_x \geq 0$ describes a set of rods parallel to x-axis and obtained as the set-theoretic intersection between slabs orthogonal to y-axis and z-axis using an R-function.

Step 3: The union of rods gives us an infinite rectangular lattice. Figure 4(a) and Figure 4(b).

$$g(x, y, z) = r_x \vee_\alpha r_y \vee_\alpha r_z \quad (7)$$

or

$$g(x, y, z) = (s_y \wedge_\alpha s_z) \vee_\alpha (s_x \wedge_\alpha s_z) \vee_\alpha (s_x \wedge_\alpha s_y) \quad (8)$$

Step 4: To obtain ellipse or circle in cross-section, offsetting operation can be used. In this case we set $l = 1$ and apply offset: Figure 4(d).

$$s_x(x, y, z) = \sin(q_x x + p_x) - 1 \quad (9)$$

$$s_y(x, y, z) = \sin(q_y y + p_y) - 1 \quad (10)$$

$$s_z(x, y, z) = \sin(q_z z + p_z) - 1 \quad (11)$$

$$r_x(x, y, z) = s_y \wedge_\alpha s_z + d_x \quad (12)$$

$$r_y(x, y, z) = s_x \wedge_\alpha s_z + d_y \quad (13)$$

$$r_z(x, y, z) = s_x \wedge_\alpha s_y + d_z \quad (14)$$

Step 5: In case d_x ,d_y, d_z are similar we obtain circle in cross-section for all the rods, otherwise we obtain ellipse.

Step 6: The formulation of a blending operation is based on the displacement added to a standard R-function, for example for the blending intersection, we have:

$$f1 \wedge_b f2 = (f1 \wedge_\alpha f2) + a_0 / (1 + (f1/a_1)^2 + (f2/a_2)^2) \quad (15)$$

where $\wedge_b$ stands for one of the R-functions defining the intersection and the additional term defines the displacement with the parameters a_0, a_1, a_2 controlling the shape of the blend. Figure 4(c).

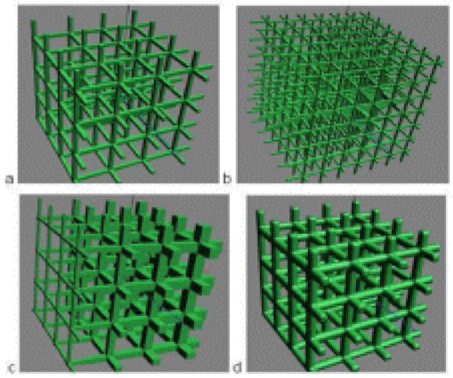

Figure 4: Function-based infinite regular lattice with (a) constant parameters; (b) double frequency (c) variable parameters – rod thickness grows linearly along one axis; (d) rods smoothed by blending .[R.2]

IV. FITTING THE LATTICE SCAFFOLD

We need to generate a lattice microstructure with the parameters obtained by means of magnetic resonance imaging for a tissue cell to be transplanted [R.5]. This is also useful for both the model adequacy analysis and the parameters estimation of the other natural and artificial objects. For lattice scaffold it is possible to design a generic parameterized

template model [R.3]. This model can later be tuned to fit the acquired data.

C. Algorithm

We investigate algorithms for fitting a parameterized scaffold model. We use a combination of a stochastic global optimization algorithm known as simulated annealing (SA) with the LevenbergMarquardt algorithm [R.2].

Step 1: initialize p, $p_{OPT} \leftarrow p$

Step 2: $G \leftarrow g(p)$, $G_{OPT} \leftarrow G$

Step 3: $T \leftarrow T0$

Step 4: $m \leftarrow 0$

Step 5: while $T > T_{min}$ **do**

Step 6: for $m = 0$ to N_T **do**

Step 7: for each parameter i **do**

Step 1: $p_{trial}[i] \leftarrow p[i] + c[i] * r$

Step 9: end for

Step 10: $G' \leftarrow g(p)$

Step 11: $\Delta E \leftarrow G' - G$

Step 12: if $\Delta E \leq 0$ **then**

Step 13: $G \leftarrow G0$

Step 14: $p \leftarrow$ ptrial

Step 15: if $G' < G_{OPT}$ **then**

Step 16: $G_{OPT} \leftarrow G$

Step 17: $p_{OPT} \leftarrow p$

Step 18: end if

Step 19: else

Step 20: $G \leftarrow G'$ with probability $e^{-\Delta E/T}$

Step 21: $p \leftarrow p_{trial}$

Step 22: end if

Step 23: end for

Step 24: $T \leftarrow r_T * T$

Step 25: end while

Step 26: $p_{OPT} \leftarrow LM(g, p_{OPT})$

Step 27: return p_{OPT}

The steps 1 to 4 initialize different variables of the algorithm: T is the variable that simulates the temperature of the system in the SA algorithm and decreases with each iteration, G keeps track of the value of the previous objective function evaluation and m defines the number of steps before a reduction of the temperature.

The combination of the initial temperature T_0, the reduction factor r_T and N_T forms the cooling schedule of the SA algorithm. In our experiments, we used the following values: $T_0 = 1000$, $r_T = 0.85$ and $N_T = 200$.

The main part of the algorithm is the loop in the steps 5 to 25. In the steps 7 to 9, a new vector of parameters is generated by adding to each parameter a random value in the range [−1, 1]. The variable c is used to limit the search space in each direction. If a parameter is outside of the search space after its modification, the step 8 is iterated one more time.

In the steps 12 to 18, if the new parameter values result in improvement they are always kept. A worst solution can still be accepted with a probability $e^{-\Delta E/T}$ (Steps 19 to 22). The best vector of parameters and the best function value found so far are also kept in steps 15 to 18. After N_T function evaluation steps, the temperature of the system is decreased (step 24), making the acceptance of worst solutions less likely. Finally, after the temperature has reached some minimal threshold the Levenberg-Marquardt algorithm is used with the best found solution p_{OPT} as an initial estimation (step 26).

D. Experimental Results

Our model has seven parameters corresponding to the scale and frequency of the slabs and the parameters of the blending Set operations. The frequency and scale of the model vary in space. They are controlled by the distance to the shell which is used to interpolate between two boundary values of the frequency and scale.

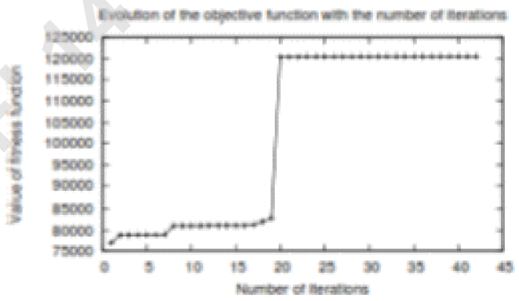

Figure 5: Evolution of the objective functions with the number of iterations.

A set of 385,535 points scattered on the surface of the object is used as the target for fitting the chosen seven parameters of the model. The termination of the main loop occurred after 42 iterations. The evolution during the algorithm's iterations of the value of the objective function corresponding to the best solution is illustrated in Figure 5. The initial values of the parameters are randomly selected: 4.513, 1.47, 1.321, 2.143, 3.632, 0.941 and 3.541. The final values are: 7.888, 2, 0.659, 0.54, 0.859, 2.003 and 3.103 corresponding respectively to the scale and frequency of the slabs (2 parameters for the scales and 2 parameters for the frequencies) and the three parameters controlling the blending union.

V. CONCLUSION

We have proposed the approach that uses periodic functions in different ways for modeling regular lattice microstructures within the FRep framework. In the case of lattices, these functions serve to directly define the point membership by analyzing the sign of the function. The proposed models are extremely compact and are implemented in HyperFun, [R.2] while providing precise and spatially

coherent models. Compared to methods using BRep, FRep parametrization provides more robust and dynamic control, including parameter-dependent changes in object's topology. The FRep models of microstructures can be used as arguments for further set-theoretic, blending, offsetting, and other geometric operations [R.6]. The primary subject of this work was modeling volumetric microstructures and it will be a subject of future research to find out if this approach can be applied to material microstructures such as grains, grain boundaries and secondary phases such as nanofibers. Finally, we intend to develop function-based models for other types of volumetric microstructures such as octahedral lattices, natural branching and organic structures.

ACKNOWLEDGMENT

The authors would like to thank Dr.Alexander Pasko for the FRep based model. We are also thankful for the support of Mrs.Renganayagi Sankarappan, Retired Chief Librarian, Dr.Jayaraman Government Theni Medical college for making this work possible by providing medical data.

REFERENCES

[1] Alan Watt, 3D Computer Graphics, 3rd ed. ISBN 0-20-139855-9.

[2] Alexander Pasko, Oleg Fryazinov, Turlif Vilbrandt, Pierre-Alain Fayolle, Valery Adzhiev Bournemouth University, UK Digital Materialization Group, Japan, and Uformia AS, Norway University of Aizu, Japan, Procedural Function-based Modeling of Volumetric Microstructures.

[3] Y. Chen, 3d texture mapping for rapid manufacturing, Computer-Aided Design & Applications 4 (6) (2008) 761-771.

[4] Hearn and Baker, Computer Graphics, C Version, 2nd ed. ISBN 0-13-530924-7.

[5] M. W. Naing, C. K. Chua, K. F. Leong, Y. Wang, Fabrication of customised scaffolds using computer-aided design and rapid prototyping techniques, Rapid Prototyping Journal 11 (4) (2005) 249–259.

[6] W. Sun, B. Starly, J. Nam, A. Darling, Bio-cad modeling and its applications in computer-aided tissue engineering, Computer-Aided Design 37 (11) (2005) 1097–1114.